Toward Efficient Chemical Potential Calculations by Expanded Ensemble Simulations; to Make the Free Energy Pathway Fairly Level

Kai Lüder and Roland Kjellander*

Department of Chemistry, Göteborg University, SE-412 96 Göteborg, Sweden

Received: February 27, 2006; In Final Form: June 4, 2006

A scheme is suggested of how to construct good bias potentials ("balancing factors") to be used in expanded ensemble (EE) calculations of chemical potentials of solutions. A combination of two strategies are used: (i) to use a pathway for particle insertions that avoids large variations in free energy and (ii) to use calculated free energy derivatives to construct a bias potential that makes the pathway fairly level. Only a few very short simulations are needed to accomplish the latter, and then, a full EE simulation is done to obtain the chemical potential. By practical calculations of the chemical potential of benzene, cyclohexane, and benzylamine in water, it is shown that this method is at least equally efficient to the recent adaptive EE (AEE) method by Åberg et al. (*J. Chem. Phys.* **2004**, *120*, 3370). Furthermore, the new method provides an alternative strategy that complements existing EE methods.

1. Introduction

Chemical potential calculations of molecules in solutions are important for many reasons. One kind of application concerns equilibrium between different phases such as in calculations of partition coefficients between various solutions, theoretical constructions of phase diagrams, and predictions of solubility. Another application is, for example, the calculation of activity factors to be used to compute ΔG for chemical reactions and for chemical equilibrium predictions. In this work, we are concerned with a method for practical calculations of chemical potentials for molecular solutes in solutions of various concentrations. All molecules are flexible and modeled by using interaction site potentials for the intermolecular interaction and, in general, more complex interaction models for the intramolecular interactions (see below).

We use the expanded ensemble (EE) simulation method by Lyubartsev et al.[1] to calculate the chemical potentials. It is a general method to calculate the free energy difference between two states of a system. We consider the insertion of a new molecule in the system. The two states then refer to the system in the absence and presence, respectively, of the new molecule. The free energy difference between the states equals the excess chemical potential for the added species. A coupling parameter α for the interaction between the added molecule and the rest of the system is introduced, and when α is increased from 0 to 1, the new particle is added "gradually" to the system. In the EE method, the coupling parameter α is considered as an extra degree of freedom in the simulation. A random walk is done in α-space as well as in particle configuration space. The free energy difference for insertion of the extra molecule is then calculated from the probabilities to visit the states of the uncoupled ($\alpha = 0$) and fully coupled ($\alpha = 1$) molecule.

For this method to be useful, one must eliminate a large part of the free energy difference between consecutive values of α, i.e., to make the free energy pathway more level. This is done by constructing a bias potential that is introduced in the exponent in the Boltzmann factor associated with the transition between consecutive α values. The bias potential depends only on α and is constructed so that the transitions can occur sufficiently easy between consecutive values of α during the EE simulation. In the original version of the EE method,[1] the bias potential (referred to as "balancing factors") is constructed by trial and error. It is changed manually until the transition probabilities become reasonable. More refined ways of doing this have appeared subsequently. In the method of Khare and Ruthledge,[2] the bias potential is constructed iteratively from the actual probabilities to visit states with different values of α during some short simulations. In the adaptive EE (AEE) method by Åberg et al.,[3] the bias potential is constructed during the simulation from the distribution of transition energies between states with consecutive values of α.

The objective of the current paper is to demonstrate another way to construct a bias potential that makes the free energy pathway fairly level so transitions occur easily. We will do this by using two strategies: (i) to use a pathway between the initial and final state that avoids large variations in free energy and (ii) to construct a bias potential that approximately eliminates the remaining free energy variations along the path. Here, we only consider molecules with intermolecular potentials that are approximated as site−site interactions using combinations of Lennard-Jones and electrostatic potentials. The strategy (i) is accomplished by turning on the Lennard-Jones and electrostatic potentials of the new particle in a balanced way when α is changed between 0 and 1. Strategy (ii) is accomplished by doing some very short simulations to calculate approximate values of the derivative of the free energy with respect to α for a small number of different α values between 0 and 1. These derivative values are used to construct the bias potential.

The optimal bias potential that would make the pathway completely flat is the free energy itself (with inverted sign) as a function of α. If this is used, states with different α values would have equal probability. In our approach, the free energy derivative values are used to construct an approximation to this optimal bias potential. If the derivatives were calculated accurately on a dense grid in α space, the optimal potential could

* Email: rkj@chem.gu.se.

10.1021/jp061245m CCC: $33.50
Published on Web 07/20/2006

be obtained by numerical integration. The latter procedure is equivalent to calculate the free energy by coupling parameter integration (a "thermodynamic integration" as it is often, but inappropriately, called in the literature). However, what is needed in an EE simulation is not the optimal bias potential; an approximation to the latter is sufficient. Thus, our method is in a way intermediate between coupling parameter integration and the usual EE method.

We will illustrate our method by doing simulations for insertion of a single solute molecule inserted in pure solvent. The method itself is, however, general and can be used for chemical potential calculations for solutions at any concentration.

2. Theory

2.1. Chemical Potential and Standard States. Let us first set up the basic definitions and equations needed for our task of designing bias potentials for chemical potential calculations. We will take the opportunity to write the equations in a form that makes it easy to see the link to the classical thermodynamic manner to handle chemical potentials of solutions. This requires very little extra work and will make it easy to connect to the selection of various standard states common in thermodynamics, a subject that is often riddled with unnecessary conceptual difficulties in applications. In particular, we will see how the standard state at infinite dilution is connected to the chemical potential we will calculate by simulation in this work.

Consider a solution of species i in a solvent consisting of species s. The chemical potential μ_i of species i is defined in the canonical ensemble as

$$\mu_i = A(N_s, N_i + 1, T, V) - A(N_s, N_i, T, V) \approx \left(\frac{\partial A}{\partial N_i}\right)_{N_s,T,V}$$

where A is Helmholtz energy, N_s and N_i are the number of solvent and solute molecules, respectively, T is the absolute temperature, and V is the volume. For a solution with molar concentration c_i (number density $n_i = N_{\mathrm{Av}}c_i$, where N_{Av} is Avogadro's constant), μ_i can generally be written as

$$\mu_i = \mu_i^0 + k_{\mathrm{B}}T \ln \frac{c_i}{c_i^0} + \mu_i^{\mathrm{ex}} \qquad (1)$$

where μ_i^0 is the standard chemical potential, k_{B} is Boltzmann's constant, c_i^0 is the concentration in the standard state, and μ_i^{ex} is the excess chemical potential. If we select the standard state as an ideal gas of species i with density n_i^0, we have $\mu_i^0 = -k_{\mathrm{B}}T \ln(q_i^0/[n_i^0\Lambda_i^3])$, where Λ_i is the thermal de Broglie wavelength of species i, and q_i^0 is the (internal) molecular partition function of an i molecule. The sum of the first two terms in the right-hand side (rhs) of eq 1 then is the chemical potential for an ideal gas of density n_i, and the excess chemical potential μ_i^{ex} of the solution contains all contributions due to the interactions between each i molecule and the rest of the system. The excess chemical potential is equal to the change in excess Helmholtz energy, A^{ex}, when adding one molecule to the solution, i.e., the reversible work against the interactions when adding the molecule. Explicitly, μ_i^{ex} is given by

$$\mu_i^{\mathrm{ex}} = A^{\mathrm{ex}}(N_s, N_i + 1, T, V) - A^{\mathrm{ex}}(N_s, N_i, T, V) = -k_{\mathrm{B}}T \ln \frac{Z_{N_s,N_i+1}}{Z_{N_s,N_i} V z_i^0} \qquad (2)$$

where Z_{N_s,N_i} is the configurational partition function (defined below) for a system with N_s solvent molecules and N_i solute molecules, and where z_i^0 is the molecular configurational partition function of a solute molecule in absence of interactions with other molecules. The numerator in the rhs of eq 2 describes a system with an additional i molecule that interacts fully with all molecules, while the denominator corresponds to a system with an additional i molecule that does not interact at all with the other molecules (a "ghost molecule").

The configurational partition functions are defined as usual. We have

$$Z_{N_s,N_i} = \int \exp[-\beta U_{N_s,N_i}(\mathbf{r}_s^{(N_s)}, \mathbf{r}_i^{(N_i)})]\, \mathrm{d}\mathbf{r}_s^{(N_s)}\, \mathrm{d}\mathbf{r}_i^{(N_i)} \qquad (3)$$

where $\beta = (k_{\mathrm{B}}T)^{-1}$, U_{N_s,N_i} is the total interactional energy (intermolecular and intramolecular) for N_s solvent molecules and N_i solute molecules, $\mathbf{r}_j^{(N_j)}$ is the full set of coordinates (intermolecular and intramolecular) for N_j molecules of species j ($j = s, i$), $\mathrm{d}\mathbf{r}_j^{(N_j)}$ is a product of the corresponding coordinate differentials, and the integrations are performed over the whole accessible space for the coordinates. The differentials of the rotational and internal coordinates (if present) of the molecules are here assumed to be properly normalized. The molecular configurational partition function is defined from

$$z_i^0 = \int \exp[-\beta u_i^{\mathrm{intra}}(\mathbf{r}_i^{\mathrm{intra}})]\, \mathrm{d}\mathbf{r}_i^{\mathrm{intra}} \qquad (4)$$

where u_i^{intra} is the intramolecular interaction energy of a single solute molecule and $\mathbf{r}_i^{\mathrm{intra}}$ is the set of its intramolecular coordinates.

The molecular partition function of the ideal gas is given by $q_i^0 = z_i^0/\lambda_i^{\mathrm{intra}}$, where $\lambda_i^{\mathrm{intra}}$ contains the contributions from the nontranslational momentum coordinates of the molecule. (If some degrees of freedom are treated quantum mechanically and are separable, these contributions are also contained in $\lambda_i^{\mathrm{intra}}$.) Thus

$$\mu_i^0 = -k_{\mathrm{B}}T \ln(z_i^0/[\lambda_i^{\mathrm{intra}} n_i^0 \Lambda_i^3]) \qquad (5)$$

Note that the concentration c_i^0 is arbitrary (c_i^0 and n_i^0 can be completely eliminated from eq 1). It is used here mainly for convenience (to make the argument of the logarithmic term dimensionless) but also because it occurs by convention in the classical thermodynamic treatments of chemical potentials of solutions. By introducing the activity factor $\gamma_i = \exp(\beta\mu_i^{\mathrm{ex}})$, we can write eq 1 as $\mu_i = \mu_i^0 + k_{\mathrm{B}}T \ln(\gamma_i c_i/c_i^0)$.

Alternatively, we can write the chemical potential in a more practical form by changing the standard state to that appropriate for an infinitely dilute solution. This is discussed in the Appendix for completeness. As shown there, the standard chemical potential for infinite dilution, $\mu_i^{\ominus}$, is given by

$$\mu_i^{\ominus} = \mu_i^0 + \mu_i^{\mathrm{ex}}(N_i{:}0 \rightarrow 1)$$

where the last term is the excess chemical potential calculated by adding one solute molecule to pure solvent. In this paper, we restrict ourselves to calculations of μ_i^{ex} at infinite dilution, but calculations of the excess chemical potential at finite concentrations can be performed by using the same methods. The only difference is whether other solute molecules are present or not in the system into which the additional solute molecule is added.

2.2. Chemical Potential in EE Simulations. We shall now introduce the coupling parameter and define the free energy

pathway that links the initial and final states when inserting a new molecule. At the same time, we will describe the expanded ensemble method and its relationship to the bias potential in a way that will suit our purpose to construct an approximation to the optimal bias potential.

The ratio $Z_{N_s,N_i+1}/Z_{N_s,N_i}Vz_i^0$ in eq 2 can be calculated by adding the extra solute molecule in a gradual manner, i.e., by gradually transforming this molecule from a ghost molecule into one that interacts fully with the other molecules. The total intermolecular interaction energy, $\tilde{u}_i^{(N_s,N_i)}$, between the extra, partially coupled molecule and the other molecules in the system (N_s solvent molecules and N_i solute molecules) are then described by a parameter α that varies between 0 and 1 such that

$$\tilde{u}_i^{(N_s,N_i)}(\mathbf{r}_s^{(N_s)}, \mathbf{r}_i^{(N_i)}; \mathbf{r}_i, \alpha) = \begin{cases} 0 & \alpha = 0 \\ u_i^{(N_s,N_i)}(\mathbf{r}_s^{(N_s)}, \mathbf{r}_i^{(N_i)}; \mathbf{r}_i) & \alpha = 1 \end{cases} \quad (6)$$

where $u_i^{(N_s,N_i)}$ is the interaction energy between a fully coupled added solute molecule with coordinates $\mathbf{r}_i$ and the other molecules with coordinates $\mathbf{r}_s^{(N_s)}$ and $\mathbf{r}_i^{(N_i)}$. (In this paper, we generally use $\tilde{u}$ to denote an α dependent potential for a partially coupled molecule and u for the corresponding potential for a fully coupled molecule.) The function $\tilde{u}_i^{(N_s,N_i)}$ must be a continuous function of α but is otherwise arbitrary for $0 < \alpha < 1$. In the current work, the parameter α does not affect the intramolecular interactions of the added molecule. The total interaction energy of the system with a partially coupled added molecule is $\tilde{U}_{N_s,N_i}(\alpha) = U_{N_s,N_i} + \tilde{u}_i^{(N_s,N_i)}(\alpha) + u_i^{\text{intra}}$. Note that $\tilde{U}_{N_s,N_i}(1) = U_{N_s,N_i+1}$, while $\tilde{U}_{N_s,N_i}(0)$ includes the intramolecular energy of a ghost molecule. Thus, $\alpha = 1$ describes the system for the numerator of the ratio $Z_{N_s,N_i+1}/Z_{N_s,N_i}Vz_i^0$ in the rhs of eq 2, while $\alpha = 0$ describes the system for the denominator.

In Monte Carlo simulations with the expanded ensemble method,[1,4] the coupling parameter α is used as an extra degree of freedom in addition to the particle coordinates. A random walk is done in all degrees of freedom including the α-space. The simulated system then has the total interaction energy $\tilde{U}_{N_s,N_i}(\alpha)$, and transitions between various particle configurations as well as between α values are performed according to the standard Metropolis algorithm. In the numerical calculations of the current paper, the change in particle coordinates for each fixed α value is, however, performed as a molecular dynamics simulation.[5,6] Only the transitions between the different α values are done with the Metropolis Monte Carlo technique.

To increase the probability for transitions between consecutive α values (or indeed, to make them at all possible in practice), one introduces a bias potential which can be described as a potential energy φ that is independent of the particle coordinates but dependent on α. Thus, φ does not affect the forces between the molecules and hence not the transitions between various particle configurations for fixed α, but it does affect the α transitions. In this approach, one makes a simulation with the total interaction energy $\tilde{U}_{N_s,N_i}(\alpha) + \varphi(\alpha)$ (the quantity $\eta(\alpha) = -\beta\varphi(\alpha)$ is often called a "balancing factor"). The configurational partition function for the system with this interaction energy will be denoted $Z^{[\varphi]}_{N_s,N_i}(\alpha)$ and is defined in analogy to eq 3. From now on, superscript $[\varphi]$ on a quantity indicates that it is calculated in the presence of the bias potential $\varphi(\alpha)$.

The probability $\mathscr{P}_i^{[\varphi]}(\alpha)$ during an EE simulation to observe the system at a certain α value is given by

$$\mathscr{P}_i^{[\varphi]}(\alpha) = \frac{Z^{[\varphi]}_{N_s,N_i}(\alpha)}{\sum_{\alpha'} Z^{[\varphi]}_{N_s,N_i}(\alpha')}$$

where the sum is over the possible values of α (these values are selected at the beginning of the simulation). The excess Helmholtz energy of the system for any α is given by

$$A_i^{[\varphi]\text{ex}}(\alpha) = A_i^{[\varphi]\text{ex}}(0) - k_B T \ln \frac{Z^{[\varphi]}_{N_s,N_i}(\alpha)}{Z^{[\varphi]}_{N_s,N_i}(0)} = A_i^{[\varphi]\text{ex}}(0) - k_B T \ln \frac{\mathscr{P}_i^{[\varphi]}(\alpha)}{\mathscr{P}_i^{[\varphi]}(0)}$$

Since the partition function in absence of the bias potential is given by $Z_{N_s,N_i}(\alpha) = Z^{[\varphi]}_{N_s,N_i}(\alpha)\exp[\beta\varphi(\alpha)]$, which follows directly from the definition, we have

$$A_i^{\text{ex}}(\alpha) = A_i^{\text{ex}}(0) - k_B T \ln \frac{\mathscr{P}_i^{[\varphi]}(\alpha)}{\mathscr{P}_i^{[\varphi]}(0)} + \varphi(0) - \varphi(\alpha)$$

In particular, we have[4]

$$\mu_i^{\text{ex}} = A_i^{\text{ex}}(1) - A_i^{\text{ex}}(0) = -k_B T \ln \frac{\mathscr{P}_i^{[\varphi]}(1)}{\mathscr{P}_i^{[\varphi]}(0)} + \varphi(0) - \varphi(1) \quad (7)$$

The bias potential $\varphi(\alpha)$ should be selected such that the transition probabilities between consecutive α values become sufficiently large so that the simulation goes between $\alpha = 0$ and 1 (passing through the intermediate values) a sufficient number of times. The optimal choice of $\varphi(\alpha)$ makes all α values equally probable, i.e., it makes all $\mathscr{P}_i^{[\varphi]}(\alpha)$ equal. This choice is given by $\varphi^{\text{opt}}(\alpha) = A_i^{\text{ex}}(0) - A_i^{\text{ex}}(\alpha)$, which means that the excess free energy differences are known—the task we set out to solve in the first place. In practice, it is enough to find a bias potential that makes every $\mathscr{P}^{[\varphi]}(\alpha)$ not too small, but one would like to come as close to $\varphi^{\text{opt}}(\alpha)$ as possible without undue effort. Here, we will suggest a new way to achieve this.

2.3. The Construction of a Suitable Bias Potential. While free energy calculations require a substantial effort, it is much easier to calculate derivatives of the free energy. In particular, we have

$$\left(\frac{\partial A_i^{\text{ex}}(\alpha)}{\partial\alpha}\right)_{N_s,N_i,T,V} = \left\langle \frac{\partial \tilde{u}_i^{(N_s,N_i)}(\mathbf{r}_s^{(N_s)}, \mathbf{r}_i^{(N_i)}; \mathbf{r}_i, \alpha)}{\partial\alpha} \right\rangle_{\text{conf}} = -\frac{\partial\varphi^{\text{opt}}(\alpha)}{\partial\alpha} \quad (8)$$

where $\langle\cdots\rangle_{\text{conf}}$ denotes the canonical ensemble average over the particle configurations of the system for the α value in question (or the time average in a molecular dynamics simulation) and where the last equality follows from the identification we made above. This expression for $\partial A_i^{\text{ex}}(\alpha)/\partial\alpha$ is commonly used in the coupling parameter integration method to calculate the chemical potential. Then, the derivative is accurately calculated on a dense mesh on the α axis and numerically integrated between $\alpha = 0$ and $\alpha = 1$. Such an integration of $\partial A_i^{\text{ex}}(\alpha)/\partial\alpha$ between 0 and α would also give $-\varphi^{\text{opt}}(\alpha)$. However, calculation of a bias potential that approximates $\varphi^{\text{opt}}(\alpha)$ requires a much smaller

effort. Such an approximation can be constructed by using $\partial\varphi^{\mathrm{opt}}(\alpha)/\partial\alpha$ values evaluated with much less precision and far fewer points than needed for the chemical potential determination. When an approximate bias potential has been determined, the accurate free energy is calculated in an EE simulation, which hence takes care of the rest.

To construct this bias potential, it is in many cases sufficient to calculate $\partial A_i^{\mathrm{ex}}(\alpha)/\partial\alpha$ for just a few α points and then interpolate to intermediate points. This interpolation can be done by, for example, fitting a spline function to the calculated values. Provided $\partial A_i^{\mathrm{ex}}(\alpha)/\partial\alpha$ varies quite smoothly for $0 < \alpha < 1$, this will give a good result even for a small number of points. Therefore, it is essential to select a coupling parameter parametrization of the interaction potentials that gives a smooth α dependence and gives balanced contributions from different kinds of interactions to the average in eq 8. (This will be discussed in section 3.3.) When the spline function for $\partial A_i^{\mathrm{ex}}(\alpha)/\partial\alpha$ is constructed, it is easy to determine the bias potential by integration.

Since we only want to have a reasonable approximation to $\varphi^{\mathrm{opt}}(\alpha)$, one can calculate the average in eq 8 by a quite short simulation for each α point. There is no need to reach a high degree of convergence—a reasonably fair convergence is enough. When one has calculated the derivative for a few points, one can, if necessary, make a judgment from the values of $\partial A_i^{\mathrm{ex}}(\alpha)/\partial\alpha$ whether some more α points are needed or not.

In this work, we will show that this method is a viable and efficient way to calculate a useful bias potential. We shall compare our method to the adaptive EE (AEE) simulation method,[3] which also provides an approximation to $\varphi^{\mathrm{opt}}(\alpha)$. In AEE, the bias potential is estimated from the observed energies of the system when a transition is made (or attempted) between consecutive α values during the EE simulation. The distributions of energy differences for the transitions involving each pair of consecutive α values are recorded. The bias potential is then determined iteratively such that the acceptance ratio for transitions from the lower to the higher α value in each pair becomes the same as for transitions in the opposite direction (for details, see ref 3).

To obtain the distribution of energy differences, from which the bias potential can be calculated in AEE, one must select the α points on a sufficiently dense grid so transitions *can* occur from the very beginning of the calculation. One may attempt to guess a starting bias potential such that transitions actually take place, but one does not know it beforehand. This puts a lower limit on how few α points one can have initially.

The main line in the current work is to show how our method can be used as an alternative to AEE and other methods to construct the bias potential and calculate μ_i^{ex}. One may, however, also consider using a combination of our method and AEE to accomplish this task. In fact, in certain cases where a very dense grid would be needed to start an AEE simulation from scratch, one can use our method to obtain information about what a good bias potential looks like and then select the grid by using this information. One can even take this a step further and construct a trial bias potential with our method and then use the AEE method for simulations on the system with this potential included. In this manner, AEE is used to *improve* the bias potential for such difficult cases as an alternative to calculating the full bias potential with our method.

2.4. Isobaric Ensemble. The EE scheme can be easily generalized to the isobaric ensemble.[4] Then, we have

$$\mu_i = G(N_s, N_i + 1, T, P) - G(N_s, N_i, T, P) \approx \left(\frac{\partial G}{\partial N_i}\right)_{N_s,T,P}$$

where G is Gibbs energy and P is the pressure. Instead of eq 2, we have

$$\mu_i^{\mathrm{ex}} = -k_{\mathrm{B}}T \ln \frac{Y_{N_s,N_i+1}}{Y_{N_s,N_i}\bar{V}z_i^0} \tag{9}$$

where $\bar{V}$ is the average volume, Y_{N_s,N_i} is the isobaric configurational partition function defined by

$$Y_{N_s,N_i}(T, P) = \frac{1}{\upsilon}\int_0^\infty Z_{N_s,N_i}(T, V)\, \mathrm{e}^{-\beta PV}\, \mathrm{d}V$$

and υ is a constant that has units of volume. The equations in the Appendix are analogously generalized. Differences in Gibbs energy can be obtained in the isobaric ensemble in analogy to the Helmholtz energy calculations discussed above by replacing canonical partitions functions, Z, with isobaric ones, Y, in the formulas. For example, the analogues to eqs 7 and 8 hold for the Gibbs energy. All methods suggested above are straightforward to implement in this case too.

3. Interactions

3.1. Site−Site Interaction Model. The intermolecular interactions are modeled as pair potentials between molecular interaction sites that have partial charges and/or are centers for Lennard-Jones interactions between the sites. Let S_j denote the set of interaction sites for a molecule of species j. The partial charge of a site s is denoted q_s, and the Lennard-Jones (LJ) parameters for interaction between sites s and t are denoted ϵ_{st} and σ_{st}. The interaction between two molecules of species j and l can be written as

$$u_{jl}^{\mathrm{pair}}(\mathbf{r}_j, \mathbf{r}_l) = \sum_{s\in S_j, t\in S_l} \{u_{st}^{\mathrm{LJ}}(r_{st}) + u_{st}^{\mathrm{Coul}}(r_{st})\} \tag{10}$$

where $\mathbf{r}_j$ is the full set of coordinates of the j molecule, $\mathbf{r}_l$ is that of the l molecule, r_{st} is the distance between sites s and t

$$u_{st}^{\mathrm{LJ}}(r) = 4\epsilon_{st}\left[\left(\frac{\sigma_{st}}{r}\right)^{12} - \left(\frac{\sigma_{st}}{r}\right)^{6}\right] \tag{11}$$

$$u_{st}^{\mathrm{Coul}}(r) = \frac{q_s q_t}{4\pi\epsilon_0 r} \tag{12}$$

and ϵ_0 is the permittivity of vacuum. In our calculations, we have assumed for simplicity that the LJ σ values between different kinds of sites are pairwise additive, $\sigma_{st} = (\sigma_{ss} + \sigma_{tt})/2$, where index *ss* and *tt* means interaction parameters between two sites of equal kind, and we have used the mixing rule for the LJ ϵ parameters, $\epsilon_{st} = (\epsilon_{ss}\epsilon_{tt})^{1/2}$. This is, of course, not necessary in general.

The atomic parameters ϵ_{ss} and σ_{ss} used for the solute molecules benzylamine (see Figure 1 and Table 1) and cyclohexane (see Table 2) are taken from the OPLS-AA (optimized potentials for liquid simulations − all atoms) force field.[7,8] The CM1A (charge model 1A) partial charges[12] are computed via single-point AM1 calculations using optimized OPLS-AA geometries and the *BOSS* program.[9−11] The obtained charges are then scaled by a factor of 1.14 to account for polarization of the solute in water.[13] Atomic parameters for benzene (see Table 3) are taken from the CHARMM force field.[14] The

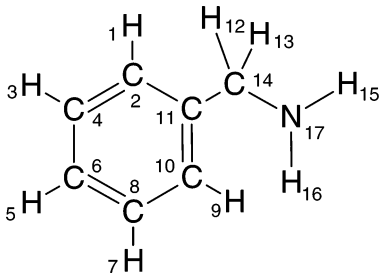

Figure 1. Atomic identities (numbers) for benzylamine in Table 1.

TABLE 1: Interaction Parameters for Benzylamine

Site−Site Interactions Parameters[a]

#	atom type	charge	ϵ (kJ/mol)	σ (Å)
1	HA	0.1555	0.1256	2.42
2	CA	−0.1291	0.2931	3.55
3	HA	0.1490	0.1256	2.42
4	CA	−0.1526	0.2931	3.55
5	HA	0.1477	0.1256	2.42
6	CA	−0.1453	0.2931	3.55
7	HA	0.1490	0.1256	2.42
8	CA	−0.1526	0.2931	3.55
9	HA	0.1555	0.1256	2.42
10	CA	−0.1291	0.2931	3.55
11	CA	−0.1023	0.2931	3.55
12	HC	0.0848	0.1256	2.50
13	HC	0.0846	0.1256	2.50
14	CT	−0.0987	0.2763	3.50
15	H	0.3898	0	0
16	H	0.3898	0	0
17	NT	−0.9930	0.7118	3.30

Bond Lengths and Force Constants of Streching

bond type	r^{eq} (Å)	$k^{(r)}$ (kJ/mol)
CA−CA	1.40	1963.61
CA−HA	1.08	1536.56
CA−CT	1.51	1327.22
CT−NT	1.448	1599.36
CT−HC	1.09	1423.51
NT−H	1.01	1817.07

Bond Angles and Force Constants of Bending

atom types	θ^{eq} (°)	$k^{(\theta)}$ (kJ/mol)
CT−NT−H	109.50	146.54
NT−CT−CA	111.20	334.94
NT−CT−HC	109.50	146.54
CT−CA−CA	120.0	293.08
CA−CA−CA	120.0	263.77
CA−CA−HA	120.0	146.54
H−NT−H	106.40	182.54
HC−CT−CA	109.50	146.54
HC−CT−HC	107.80	138.16

Bond Torsion Coefficients[a]

atom types	$k_{m=1}^{(\phi)}$ (kJ/mol)	$k_{m=2}^{(\phi)}$ (kJ/mol)	$k_{m=3}^{(\phi)}$ (kJ/mol)
CA−CT−NT−H	−0.795	−1.746	1.750
HC−CT−NT−H	0	0	1.675
other torsions[b]	0	30.354	0
improper torsions[c]	0	9.211	0

[a] See Figure 1 for atom numbers. [b] CA-CA-CA-CT, HA-CA-CA-CA, HA-CA-CA-CT, HA-CA-CA-HA, and CA-CA-CA-CA. [c] Atoms 2−11−14−10, 9−10−11−8, 7−8−10−6, and 5−6−8−4.

primary objective of this paper is to test the efficiency of the chemical potential calculation method, so the values of the interaction parameters are not of critical importance.

3.2. Intramolecular Interactions. The intramolecular interaction energy of a j molecule is $u_j^{\text{intra}}(\mathbf{r}_j^{\text{intra}})$, where the intramolecular coordinates $\mathbf{r}_j^{\text{intra}}$ are contained in the set of particle coordinates $\mathbf{r}_j$. In our calculations, the intramolecular interactions are modeled as sums of terms describing the energy contributions that depend on bond lengths, U^{bond}, bond angles, U^{bend}, and torsional angles, U^{torsion}

TABLE 2: Interaction Parameters for Cyclohexane

Site−Site Interaction Parameters

atom type	charge	ϵ (kJ/mol)	σ (Å)
CT	−0.1732	0.2763	3.50
HC	0.0866	0.1256	2.50

Bond Lengths and Force Constants of Streching

bond type	r^{eq} (Å)	$k^{(r)}$ (kJ/mol)
CT-CT	1.529	1122.12
CT-HC	1.090	1423.58

Bond Angles and Force Constants of Bending

atom types	θ^{eq} (°)	$k^{(\theta)}$ (kJ/mol)
CT-CT-CT	112.70	244.31
CT-CT-HC	110.70	157.01
HC-CT-HC	107.80	138.17

Bond Torsion Coefficients

atom types	$k_{m=1}^{(\phi)}$ (kJ/mol)	$k_{m=2}^{(\phi)}$ (kJ/mol)	$k_{m=3}^{(\phi)}$ (kJ/mol)
CT-CT-CT-CT	5.4431	−0.2094	0.8374
CT-CT-CT-HC	0	0	1.2561
HT-CT-CT-HC	0	0	1.2561

TABLE 3: Interaction Parameters for Benzene

Site−Site Interaction Parameters

atom type	charge	ϵ (kJ/mol)	σ (Å)
CA	−0.1410	0.2930	3.549
HP	0.1410	0.1260	2.420

Bond Lengths and Force Constants of Stretching

bond type	r^{eq} (Å)	$k^{(r)}$ (kJ/mol)
CA-CA	1.375	1277.0
CA-HP	1.080	1423.0

Bond Angles and Force Constants of Bending

atom types	θ^{eq} (°)	$k^{(\theta)}$ (kJ/mol)
CA-CA-CA	120.0	167.50
CA-CA-HP	120.0	125.60

Bond Torsion Coefficients[a]

atom types	$k_{m=2}^{(\phi)}$ (kJ/mol)
CA-CA-CA-CA	13.0
CA-CA-CA-HP	17.6
HP−CA-CA-HP	10.0

[a] $k_m^{(\Phi)} = 0$ for $m = 1$ and 3.

$$U_{st}^{\text{bond}}(r_{st}) = k_{st}^{(r)}(r_{st} - r_{st}^{\text{eq}})^2 \tag{13}$$

$$U_{stt'}^{\text{bend}}(\theta) = k_{stt'}^{(\theta)}(\theta_{stt'} - \theta_{stt'}^{\text{eq}})^2 \tag{14}$$

$$U_{s'stt'}^{\text{torsion}}(\phi_{s'stt'}) = \sum_{m=1}^{3} k_{m,s'stt'}^{(\phi)}[1 + \cos(m\phi_{s'stt'} - \vartheta_{m,s'stt'}^{0})]/2 \tag{15}$$

where s', s, t, and t' are covalently linked atomic sites in a molecule, $k_{st}^{(r)}$, $k_{stt'}^{(\theta)}$, and $k_{s'stt'}^{(\phi)}$ are constants, $\theta_{stt'}$ is a bond angle, $\phi_{s'stt'}$ is angle between the planes $s'st$ and stt', r_{st}^{eq} and $\theta_{stt'}^{\text{eq}}$ are equilibrium values, and $\vartheta_{m,s'stt'}^{0}$ is a phase constant (in our

calculations, the latter is 0 for $m = 1$, 3 and 180° for $m = 2$). $U_{s's tt'}^{\text{torsion}}$ is also applied for "improper torsions", for which the site t' is bonded to s rather than to t. The values of the interaction parameters in eqs 13−15 for benzylamine and cyclohexane are taken from the OPLS-AA force field;[7,8] see Tables 1 and 2. For benzene, they are taken from the CHARMM force field;[14] see Table 3. In addition to these interactions, there are intramolecular interaction terms with the potential $u_{st}^{\text{LJ}}(r_{st}) + u_{st}^{\text{Coul}}(r_{st})$ for sites that are not covalently linked ("nonbonded interactions"). The same interaction parameters are used for the nonbonded intramolecular and the intermolecular interactions.

The water molecules are modeled using a flexible SPC (single point charge) model with an anharmonic Morse potential for the description of the O−H bond stretches.[15] This model gives a dielectric constant and diffusion coefficient in good agreement with experiments.[16]

The total energy of the system is the sum of intramolecular energies for all molecules and the intermolecular interaction energies between all pairs of molecules in the system.

3.3. Balanced Coupling Parameter Choice. When the extra i molecule is added by gradually increasing its coupling to all other molecules in accordance with the condition in eq 6, the α dependence for $0 < \alpha < 1$ can be selected in various ways. In EE simulations, it is common to use a linear α dependence, $\tilde{u}_i^{(N_s,N_i)}(\alpha) = \alpha u_i^{(N_s,N_i)}$. Then, in the calculation of $\tilde{u}_i^{(N_s,N_i)}(\alpha)$, one uses the pair interaction

$$\tilde{u}_{il}^{\text{pair}}(\mathbf{r}_i, \mathbf{r}_l; \alpha) = \sum_{s\in S_i, t\in S_l} \alpha\{u_{st}^{\text{LJ}}(r_{st}) + u_{st}^{\text{Coul}}(r_{st})\} \quad \text{(linear coupling)} \quad (16)$$

where $\mathbf{r}_i$ is the set of coordinates of the added molecule and $\mathbf{r}_l$ that of another molecule. We obtain $\tilde{u}_i^{(N_s,N_i)}(\alpha)$ by summing $\tilde{u}_{il}^{\text{pair}}(\mathbf{r}_i, \mathbf{r}_l; \alpha)$ over the N_s solvent molecules and N_i solute molecules already present, where $\mathbf{r}_l$ assumes, in turn, the coordinate values of each of these molecules.

Since the site−site interaction potentials become infinite when $r_{st} \to 0$, the linear coupling leads to the well-known singularity problem at the origin for small $\alpha > 0$.[17,18] Irrespectively of how small the α value is for $\alpha > 0$, the molecules will experience very large potentials when $r_{st} \approx 0$. This usually leads to poor numerical accuracy due to large fluctuations. Furthermore, the optimal bias potential has a huge derivative near $\alpha = 0$. In AEE calculations, this can usually be dealt with by using an extremely dense α grid for small α values.[3]

The singularity problems can be avoided[17] by replacing r in eq 11 by a shifted value $r + b(1 - \alpha)$, where the value of b in general is different for each kind of pair of sites. Then, the LJ potential at $r = 0$ is finite when $\alpha < 1$. The analogous thing can be done in eq 12, and one may in general use a prefactor α^ν with $\nu \geq 1$ instead of α and a factor $(1 - \alpha)^{\nu'}$ with $\nu' \geq 1$ in the expression for the r shift (cf. for example ref 18 where more complicated expressions are used for the α parametrization).

When designing a parametrization, one had better avoid an unmotivated imbalance between the LJ and Coulomb potentials when α is decreased from 1. Such imbalances can occur since the r dependence of the two kinds of potentials are very different. One would like to have an α parametrization such that the contributions from the LJ and Coulomb potentials just vanish when α goes to zero without any one of the contributions taking over too much before zero is reached. There are many more or less complicated ways to accomplish this. For molecules with many interaction sites, it is important that the parametrization is relatively straightforward to implement without many parameters that have to be adjusted to avoid problems.

In this work, we suggest a simple way to make the α dependence balanced, so one can quite easily control the contributions from the LJ and Coulomb potentials to the excess chemical potential. We take

$$\tilde{u}_{st}^{\text{LJ}}(r; \alpha) = 4\epsilon_{st}\left[\left(\frac{\sigma_{st}}{r + b_{st}(1-\alpha)}\right)^{12} - \left(\frac{\sigma_{st}}{r + b_{st}(1-\alpha)}\right)^{6}\right] \quad (17)$$

$$\tilde{u}_{st}^{\text{Coul}}(r; \alpha) = \frac{q_s q_t}{4\pi\epsilon_0[r + b_{st}(\alpha^{-1} - \alpha)]} \quad (18)$$

and

$$\tilde{u}_{il}^{\text{pair}}(\mathbf{r}_i, \mathbf{r}_l; \alpha) = \sum_{s\in S_i, t\in S_l} \alpha^\nu\{\tilde{u}_{st}^{\text{LJ}}(r_{st}; \alpha) + \tilde{u}_{st}^{\text{Coul}}(r_{st}; \alpha)\} \quad (19)$$

Note that the b_{st} parameters are the same for the LJ and Coulomb potentials (suitable values of these parameters will be selected below). The Coulomb potential is shifted by $b_{st}(\alpha^{-1} - \alpha)$, which makes the singular point of this potential to go to $r = -\infty$ when $\alpha \to 0$ and $\tilde{u}_{st}^{\text{Coul}}$ becomes identically zero for all r when $\alpha = 0$. The factor α^ν in eq 19 makes the remaining interaction contributions to vanish in $\tilde{u}_{il}^{\text{pair}}$ when $\alpha = 0$.

Equation 8 implies that $\partial A_i^{\text{ex}}(\alpha)/\partial\alpha$ with this choice of pair potentials equals

$$\frac{\partial A_i^{\text{ex}}(\alpha)}{\partial\alpha} = \sum_l \sum_{\text{molecules}} \sum_{s\in S_i, t\in S_l}\Bigg[\nu\alpha^{\nu-1}\langle\tilde{u}_{st}^{\text{LJ}}(r_{st}; \alpha) + \tilde{u}_{st}^{\text{Coul}}(r_{st}; \alpha)\rangle_{\text{conf}} + \alpha^\nu\left\langle\frac{\partial\tilde{u}_{st}^{\text{LJ}}(r_{st}; \alpha)}{\partial\alpha} + \frac{\partial\tilde{u}_{st}^{\text{Coul}}(r_{st}; \alpha)}{\partial\alpha}\right\rangle_{\text{conf}}\Bigg] \quad (20)$$

where the first two sums are over all molecules (except the inserted one) of all species (l) and S_i is the set of sites for the inserted i molecule. Hence, when $\alpha \to 0$, we have

$$\frac{\partial A_i^{\text{ex}}(\alpha)/\partial\alpha}{\alpha^{\nu-1}} \to \nu\sum_l n_l \sum_{s\in S_i, t\in S_l} \int \tilde{u}_{st}^{\text{LJ}}(r; 0)\, \mathrm{d}\mathbf{r} \quad (21)$$

where we have used the fact that the molecules in the solution are uniformly distributed when $\alpha = 0$ (since they do not interact with the added i molecule, a ghost molecule). Thus, in our choice of α parametrization, the integral of $\tilde{u}_{st}^{\text{LJ}}$ for $\alpha = 0$ determines how fast $A^{\text{ex}}(\alpha)$ approaches $A^{\text{ex}}(0)$ when $\alpha \to 0$. The value of $\partial A_i^{\text{ex}}(\alpha)/\partial\alpha$ for $\alpha = 0$ is zero when $\nu > 1$, and for $\nu = 1$, it is given by the rhs of eq 21. No simulation is needed to determine this value.

For $\alpha = 1$, the value of $\partial A_i^{\text{ex}}(\alpha)/\partial\alpha$ for *all* ν *and* b_{st} *values* can be determined from one single simulation (as we shall see, the simulation can be quite short to obtain good estimates of the derivative). We have from eq 20

$$\left.\frac{\partial A_i^{\text{ex}}(\alpha)}{\partial\alpha}\right|_{\alpha=1} = \sum_l \sum_{\text{molecules}} \sum_{s\in S_i, t\in S_l} [\nu\langle u_{st}^{\text{LJ}}(r_{st}) + u_{st}^{\text{Coul}}(r_{st})\rangle_{\text{conf};\alpha=1} - b_{st}\langle u'^{\text{LJ}}_{st}(r_{st}) + 2u'^{\text{Coul}}_{st}(r_{st})\rangle_{\text{conf};\alpha=1}]$$

where the sums mean the same as in eq 20 and $u'(r)$ denotes $\mathrm{d}u(r)/\mathrm{d}r$. Thus, even before the values of ν and b_{st} are

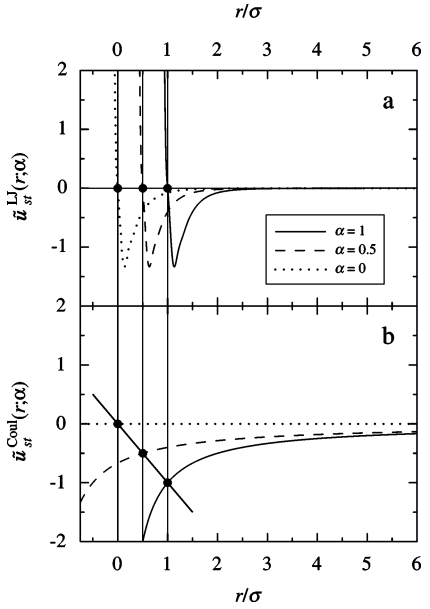

Figure 2. Illustration of the coupling parameter dependence of (a) the Lennard-Jones and (b) the electrostatic site−site interaction terms ($\tilde{u}_{st}^{LJ}$ and $\tilde{u}_{st}^{Coul}$, respectively) for our balanced α parametrization shown in eqs 17 and 18. The figures show the special case $b_{st} = \sigma_{st}$ used in the calculations in this work. When α is decreased, the origin of $\tilde{u}_{st}^{LJ}$ is shifted to the left linearly with α, while the origin of $\tilde{u}_{st}^{Coul}$ is shifted much faster, so it approaches $r = -\infty$ when $\alpha \to 0$. For $\alpha = 0$, the repulsive part of $\tilde{u}_{st}^{LJ}$ is absent for $r > 0$ in this case, and $\tilde{u}_{st}^{Coul} \equiv 0$. The points where $\tilde{u}_{st}^{LJ}$ is zero (filled circles in (a)) correspond to values of $\tilde{u}_{st}^{Coul}$ (filled circles in (b)) that vary linearly with α as indicated by the tilted straight line through the origin. The sum of $\tilde{u}_{st}^{LJ}$ and $\tilde{u}_{st}^{Coul}$ is multiplied by α^{ν} in the total pair interaction potential as shown in eq 19.

determined, we can get information for both $\alpha = 0$ and $\alpha = 1$ about how $\partial A_i^{ex}(\alpha)/\partial\alpha$ depends on these two parameters. This can be of help when designing the free energy pathway by selecting suitable ν and b_{st} for all pairs of sites s and t.

To see how our parametrization makes the LJ and Coulomb potential balanced in the pair potential, let us consider the value of $\tilde{u}_{st}^{LJ}$ at $r = r'$ for the fully coupled molecule ($\alpha = 1$), i.e., $4\epsilon_{st}[(\sigma_{st}/r')^{12} - (\sigma_{st}/r')^{6}]$. When $\alpha < 1$, the function $\tilde{u}_{st}^{LJ}$ will assume this particular value for $r = r' - b_{st}(1 - \alpha)$, a simple coordinate shift in r space. The Coulomb potential for this r value is

$$\tilde{u}_{st}^{Coul}(r' - b_{st}(1-\alpha); \alpha) = \frac{q_s q_t}{4\pi\epsilon_0[r' + b_{st}(\alpha^{-1} - 1)]}$$

which goes monotonically to zero when $\alpha \to 0$, while the LJ potential for the same r value stays constant. Thus, the Coulomb potential will decrease in magnitude everywhere relative to the LJ potential when α decreases.

Furthermore, consider the value of $\tilde{u}_{st}^{LJ}$ at the origin when $\alpha = 0$, i.e., $4\epsilon_{st}[(\sigma_{st}/b_{st})^{12} - (\sigma_{st}/b_{st})^{6}]$. (This corresponds to a special case: $r' = b_{st}$ above.) When $\alpha \neq 0$, the function $\tilde{u}_{st}^{LJ}$ assumes this particular value when $r = \alpha b_{st}$. The Coulomb potential for this r is

$$\tilde{u}_{st}^{Coul}(\alpha b_{st}; \alpha) = \frac{\alpha q_s q_t}{4\pi\epsilon b_{st}}$$

which goes linearly to zero when $\alpha \to 0$. In Figure 2, we have shown an example where we have selected $b_{st} = \sigma_{st}$ so $\tilde{u}_{st}^{LJ}$ is zero at the origin when $\alpha = 0$. For $\alpha > 0$, the value of the Coulomb potential for the r value where $\tilde{u}_{st}^{LJ}$ is zero depends linearly on α as indicated by the tilted straight line through the origin. Analogous curves would apply for other choices of b_{st}. These are the key features of the parametrization, which make the Coulomb potential go away in a manner that is globally balanced relative to the LJ potential when α is decreased.

One should avoid having $b_{st} < \sigma_{st}$, since the repulsive part of the LJ potential then remains exposed for α near zero and can quickly give large contributions when α is increased. Note, however, that if we select $b_{st} = \sigma_{st}(2/33)^{1/6} \approx 0.627\sigma_{st}$, the rhs of eq 21 is equal to zero, so $\partial A_i^{ex}(\alpha)/\partial\alpha$ is zero for $\alpha = 0$ even when $\nu = 1$. In some cases, this may be a suitable choice, but one should note that with this choice there can be numerical difficulties to evaluate $\partial A_i^{ex}(\alpha)/\partial\alpha$ for small α values, since there is a large (but finite) positive contribution from the LJ interaction term in a region around the origin. The molecules are, however, not prevented from entering into this region when α is small, since the interaction potential in eq 19 has a factor of α in front. This can lead to large fluctuations when the average is calculated.

In this work, we have selected $b_{st} = \sigma_{st}$ and $\nu = 1$, and then, $\partial A_i^{ex}(\alpha)/\partial\alpha$ for $\alpha = 0$ is slightly negative. As we shall see, this is a suitable choice for the systems that we study.

In many parametrization schemes, problems may occur when $\alpha \to 0$ if the system contains molecules that have some interaction site with only a partial charge but no LJ potential centered at the same site. For $\alpha = 1$, the charges are generally "protected" by a LJ potential from some neighboring site, i.e., the charge is prevented from overlapping with a charge of opposite sign by the repulsion from the LJ potential from the neighboring site. However, if the α parametrization is not well-designed, the protection will disappear when α is decreased, and huge Coulomb interactions will appear.

Our parametrization scheme will work without problems in these cases provided the b_{st} value of the protecting site is used as b_{st} value in eq 18 for the site with only a partial charge. To see this, we write the square bracket in the denominator of eq 18 as $[r + b_{st}(1 - \alpha) + b_{st}(\alpha^{-1} - 1)]$. The term $b_{st}(1 - \alpha)$ provides a coordinate shift for the Coulomb potential that is the same as for the protecting LJ potential, and the term $b_{st}(\alpha^{-1} - 1)$ shifts it further. This diminishes the Coulomb potential compared to the LJ potential, so the charge remains protected by the LJ repulsion for all α values.

4. Computational Methods

The simulations performed in this work were done with the expanded ensemble simulation program developed by Luybartsev et al.[5,6] Sampling of configuration space for each individual α value was done by molecular dynamics, while the Metropolis Monte Carlo acceptance rule was used for the transitions between consecutive α values.

All simulations were performed in the isobaric−isothermal (NPT) ensemble at 298 K and 1.00 atm. A Nosé−Hoover[19,20] thermostat and barostat were used to keep the temperature and pressure constant during simulations. A cubic simulation cell was used that contained 255 SPC water molecules and one solute molecule. Periodic boundary conditions were applied, and the cutoff distance r_c for the LJ interactions was set to half the simulation box length. The LJ forces were set to zero for $r > r_c$. The LJ energies and the contribution of LJ interactions in the pressure were adjusted with a tail correction term where the radial distribution function is set to one beyond r_c. The

electrostatic interactions between the molecules were calculated using the Ewald summation method.[21] All molecules were flexible and had varying bond lengths, bond angles, and torsions angles.

Since the forces between the various atoms of the molecules fluctuate at different time scales, a multiple (double) time step algorithm by Tuckerman et al.[22] was used (see also ref 5). A time step of 0.2 fs was employed for the intramolecular interaction contributions involving bond lengths, bond angles, torsional angles, or nonbonded atoms within a distance of 5 Å from each other. For the other intramolecular interactions, the time step was 2.0 fs. For intermolecular forces, the time step was also 0.2 fs for molecules with distances less than 5 Å from each other and 2.0 fs otherwise.

The start configuration for water was taken from a converged simulation of 255 water molecules after 4 ns. At the start of the simulation, we selected $\alpha = 0$ so the solute is represented inside the equilibrated water system as a "ghost molecule".

The original program by Luybartsev et al. has been modified to implement (i) the coupling parameter dependence as shown in eqs 17−19 and (ii) the calculation of $\partial A_i^{ex}(\alpha)/\partial\alpha$. Since Ewald summation is used for the electrostatic interactions, we use a slightly modified α dependence compared to eq 18. The shift in origin by $b_{st}(\alpha^{-1} - \alpha)$ is employed only for the real space component of the Ewald sum, while the contribution from the Fourier space component, that varies slowly in real space, is not shifted. The electrostatic interaction given by the total Ewald sum is then multiplied by α^{ν} as shown in eq 19.

The efficiency of EE free energy calculations depends on the number of α grid points between $\alpha = 0$ and $\alpha = 1$, as discussed by Luybartsev et al.[4] If one has too few α points, the acceptance rate for the transitions between adjacent α values will be too low, and this will cause large statistical errors. Too many grid points, on the other hand, makes the frequency of visiting the end states, $\alpha = 0$ and $\alpha = 1$, too low. This will cause large statistical errors for $\mathscr{P}_i^{[\varphi]}(0)$ and $\mathscr{P}_i^{[\varphi]}(1)$ in eq 7. In both cases, the simulation time has to be unnecessarily long to obtain a good accuracy. The optimal number of α grid points required to obtain an efficient free energy calculation with minimal statistical errors is system-dependent and is usually not known in advance. Since our method yields the approximate free energy between $\alpha = 0$ and $\alpha = 1$, one is free to choose any number of grid points with known bias potential values. It is then easy to increase or decrease the number of grid points as needed to obtain a good efficiency.

5. Results and Discussion

Results for the chemical potential and the bias potential $\varphi(\alpha)$ calculated with the new method will be presented for three different systems. The computational efficiency to estimate near-optimal bias potentials is compared with the AEE method. Three different systems were studied: cyclohexane, benzene, and benzylamine in aqueous solution at infinite dilution. These systems were chosen to represent a strongly hydrophobic molecule, a less hydrophobic molecule, and a molecule with a polar group. Benzene in water has been frequently studied by simulations over the years. Simulation results for cyclohexane in water are also frequently found in the literature. For benzylamine in water, not so frequently studied, results have, for example, been reported by Åberg, Lyubartsev, and co-workers[3,23] with EE/AEE simulations. Our primary objective here is, however, to test our method and not to obtain new chemical potential values.

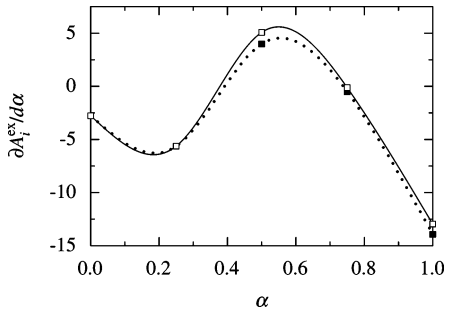

Figure 3. Approximate free energy derivative $\partial A_i^{ex}(\alpha)/\partial\alpha$ for benzene in water. The figure shows spline function fits (curves) to the approximately calculated values of the derivative (symbols) for a few values of the coupling parameter α. The total simulation time is 244 ps (full line and open squares) or 124 ps (dotted line and filled squares). The symbols for the data points at $\alpha = 0$ and 0.25 are overlapping.

The derivative $\partial A_i^{ex}(\alpha)/\partial\alpha$ was calculated in short simulations for five coupling parameter values, $\alpha = 0$, 0.25, 0.50, 0.75, and 1.0 in our coupling scheme (eqs 17−19) with $\nu = 1$ and $b_{st} = \sigma_{st}$. The derivative value at $\alpha = 0$ is known analytically, cf. eq 21, and need not be calculated by simulation, but we have nevertheless done so to test the accuracy of the simulation. From these five $\partial A_i^{ex}(\alpha)/\partial\alpha$ values, a curve was constructed by a cubic spline interpolation that gives the function for all α as shown for benzene in Figure 3 for two cases with total simulation times of 124 and 244 ps, respectively. The simulation times for the different α values in the latter case were set to 2 ps for $\alpha = 0$ and 0.25, 40 ps for $\alpha = 0.50$, 80 ps for $\alpha = 0.75$, and 120 ps for $\alpha = 1.0$. In the 124 ps case, the latter three simulation times were halved. No equilibration was performed when changing from one α value to another in the simulation.

The approximate $A_i^{ex}(\alpha)$ value for any α is calculated by analytic integration of the obtained spline function for $\partial A_i^{ex}(\alpha)/\partial\alpha$. The function $-\Delta A_i^{ex}(\alpha) = A_i^{ex}(0) - A_i^{ex}(\alpha)$ is then used as a bias potential $\varphi(\alpha)$ in EE simulations. The approximate $\Delta A_i^{ex}(\alpha)$ curves for benzene are shown in Figure 4a for the cases 124 and 244 ps. In the figure, they are compared with the converged result for $\Delta A_i^{ex}(\alpha)$ from an EE simulation. The corresponding results for benzylamine and cyclohexane are shown in Figure 4b,c. For all three systems, the approximate curves are in acceptable agreement with the converged results. This shows that $\varphi(\alpha)$ can be taken from the approximate $\Delta A_i^{ex}(\alpha)$ values and then be used in EE simulations. The results from the 124 ps simulations are sufficiently good for our purposes.

In Figure 5, we have compared the approximate $\Delta A_i^{ex}(\alpha)$ values for cyclohexane obtained with our method and the corresponding values from the AEE method after equal total simulation times, i.e., 124 and 244 ps (the coupling is given by eqs 17−19 in all cases). The results show that our method gives about the same overall accuracy as the AEE method. One can also see that already after 124 ps a fair approximation of the free energy is obtained with both methods. The corresponding results for benzene and benzylamine (not shown) are similar to those in Figure 5. This shows that our method to construct $\varphi(\alpha)$ via the calculations of the derivatives for a few α values is a viable alternative.

It is of interest to compare the free energy pathway for our balanced α parametrization, eqs 17−19, with the corresponding pathway for the linear α dependence, eq 16, that has been commonly used in EE simulations.[1,3,5,23] Figure 6a shows converged results for $\Delta A_i^{ex}(\alpha)$ from the linear parametrization

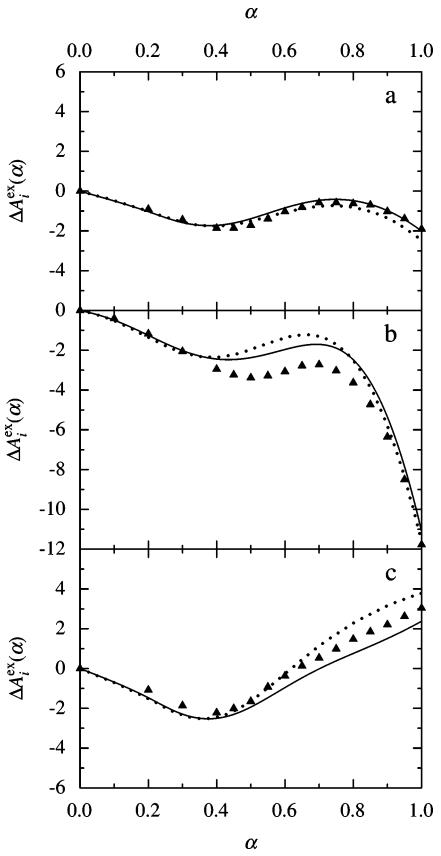

Figure 4. The variation of excess free energy $\Delta A_i^{ex}(\alpha) = A_i^{ex}(\alpha) - A_i^{ex}(0)$ with coupling parameter α for (a) benzene, (b) cyclohexane, and (c) benzylamine in water. The symbols (filled triangles) show the converged simulation results, while the curves show the integrated spline function fits to the approximate derivative from 244 ps (full line) and 124 ps (dotted line) simulations.

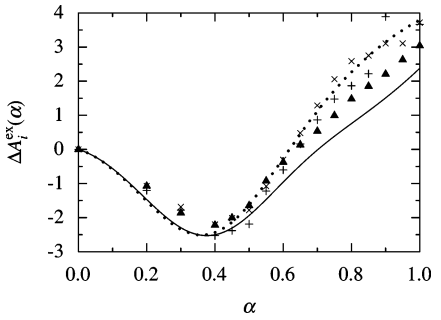

Figure 5. Same as Figure 4c, but with AEE results from 244 ps (×) and 124 ps (+) simulations also included.

for the three different solutes, and Figure 6b shows the corresponding curves for our balanced parametrization. The curves in Figure 6a have a very steep rise in the region of small α values caused by the repulsive term in the LJ potential ($\Delta A_i^{ex}(\alpha)$ then has an infinite derivative for $\alpha = 0$). This very fast increase makes it necessary to select consecutive α grid points on a logarithmic scale for small α values. Calculations of accurate values of $\partial A_i^{ex}(\alpha)/\partial\alpha$ are, of course, difficult for $\alpha > 0$ in this region and are computationally expensive, so our scheme to obtain bias potentials is unsuitable here. In the region of larger α values where the free energy pathway is more smooth, the consecutive α values can be chosen on a linear scale. The curves in Figure 6b show that the free energy pathways are smoother everywhere for our balanced α parametrization. Sufficiently accurate $\partial A_i^{ex}(\alpha)/\partial\alpha$ can in this case be obtained from short simulations as seen above.

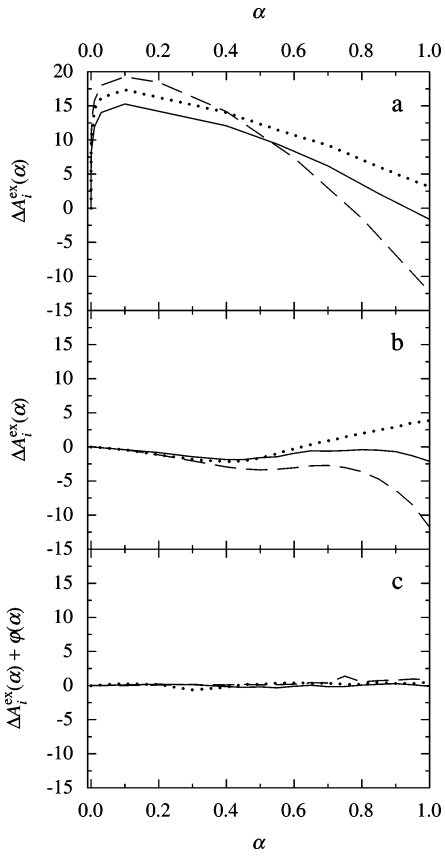

Figure 6. The free energy pathway, i.e., the excess free energy $\Delta A_i^{ex}(\alpha)$ as a function of α, for benzene (full line), cyclohexane (dotted line), and benzylamine (dashed line) in water for various cases: (a) linear coupling parametrization, eq 16; (b) balanced coupling parametrization, eqs 17−19, with $\nu = 1$ and $b_{st} = \sigma_{st}$; and (c) the same parametrization as in (b) but in the presence of bias potential $\varphi(\alpha)$ calculated with our procedure. In the latter case, $\varphi(\alpha)$ is set equal to the approximate $\Delta A_i^{ex}(\alpha)$ obtained from the 244 ps derivative calculation shown in Figure 4; see text.

Figure 6c shows the actual free energy pathway, $\Delta A_i^{ex}(\alpha) + \varphi(\alpha)$, that we have in the presence of our bias potential for the balanced α parametrization. The pathway is nearly level for all three systems, so we are quite close to using the optimal bias potential in our simulations. The sensitivity of the use of different $\varphi(\alpha)$ in EE simulations is illustrated in Figure 7 for benzylamine, where we investigate the convergence of μ^{ex} with simulation time for $\varphi^{opt}(\alpha)$ and for $\varphi(\alpha)$ obtained with our method after 124 and 244 ps simulation time, respectively (i.e., when we set $\varphi(\alpha) = -\Delta A_i^{ex}(\alpha)$ using the values for the free energy from Figure 4c). The results in Figure 7 illustrate that the accuracy of $\varphi(\alpha)$ is not critical in the EE simulation, and converged results are obtained after about 1700 ps in all three cases (for $\varphi^{opt}(\alpha)$ the convergence is, perhaps, a little bit faster than the other two). The corresponding results for benzene (not shown) look similar to those in Figure 7. For cyclohexane (not shown), the results are not fully converged at 3000 ps for any of the three choices of $\varphi(\alpha)$, but the deviations in the final result are quite small.

We can conclude that our method is as good as the AEE method in constructing $\varphi(\alpha)$. One advantage with our method compared to the AEE method is that one is free to select any number of α grid points in the EE simulation once $\partial A_i^{ex}(\alpha)/\partial\alpha$

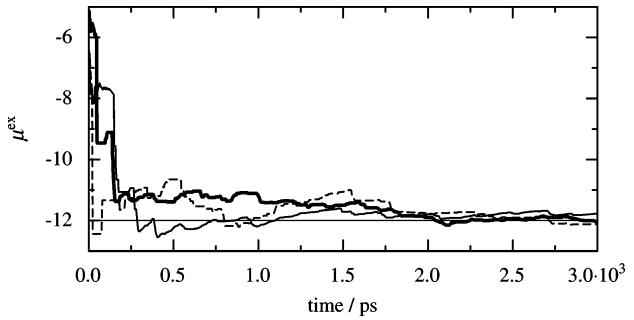

Figure 7. Investigation of the convergence with simulation time for the excess chemical potential, μ_i^{ex}, for benzylamine in water when different bias potentials have been used. Thin full line: simulation with optimal bias potential $\varphi^{opt}(\alpha)$, Thick full line: with $\varphi(\alpha)$ from 244 ps derivative calculation. Dashed line: with $\varphi(\alpha)$ from 124 ps derivative calculation. In the first case, $-\varphi(\alpha)$ is set equal to the converged $\Delta A_i^{ex}(\alpha)$ from a 3000 ps AEE simulation, while in the latter two cases, it is set equal to the approximate $\Delta A_i^{ex}(\alpha)$ shown in Figure 4c obtained from derivative calculation by short simulations (see text).

has been calculated for a few α values. In AEE, one must select a sufficient number of grid points initially, so the transitions in α can take place in absence of a bias potential (or with a guessed such potential). This number of points is not necessarily the optimal number for efficient EE simulation in the presence of the bias potential. If one initially has selected too few α grid points in the AEE method, one has to restart the simulation with more points. Furthermore, in our method one obtains information about how the free energy pathway looks before the EE simulation is started, which is quite useful when selecting the α points. If necessary, one can complement with derivative values at more grid points if this is needed to construct a good spline approximation for the free energy in more complicated cases.

Since there exists a minimal number of α points in the EE simulation to obtain a fair probability for visiting the end values $\alpha = 0$ and $\alpha = 1$ even when one has a completely flat free energy pathway (i.e., in the presence of $\varphi^{opt}(\alpha)$), it is necessary to obtain further information about the path to find nearly optimal placements of the grid points. For example, the enthalpy and entropy pathways may be less smooth than the free energy one, and information about these entities can be of value when selecting α points. The variation in enthalpy and entropy with α can also be extracted from the short simulations for the few α values where $\partial A_i^{ex}(\alpha)/\partial\alpha$ is calculated.

6. Conclusions

We have suggested a method to construct good bias potentials ("balancing factors") to be used in chemical potential calculations of solutions by expanded ensemble simulations. The method uses a coupling parameter pathway that avoids large variations in free energy, and a bias potential is constructed that approximately eliminates the remaining free energy variations along the path. It is shown in practical EE calculations that our method is at least equally efficient as the recent AEE method. One advantage of our method is that the bias potential is constructed before the EE simulation starts, which makes it possible to select the grid points in α space in a manner that is suitable for the system. Several other advantages of the pathway construction are pointed out in the paper.

Acknowledgment. This work was supported by the Swedish Research Council.

Appendix

For completeness, we show here how the chemical potential is expressed relative to a standard state of infinitely dilute solution. We have

$$\mu_i = \mu_i^{\ominus} + k_B T \ln \frac{c_i}{c_i^0} + \mu_i^{ex\ominus} = \mu_i^{\ominus} + k_B T \ln \frac{\gamma_i^{\ominus} c_i}{c_i^0} \quad (22)$$

where $\mu_i^{\ominus}$ is the standard chemical potential of species i in an infinitely dilute solution, $\mu_i^{ex\ominus}$ is the excess chemical potential relative to this standard state, and $\gamma_i^{\ominus}$ is the corresponding activity factor. In this case, we take $\mu_i^{\ominus} = -k_B T \ln[z_i^{\ominus}/(\lambda_i^{intra} n_i^0 \Lambda_i^3)]$, where

$$z_i^{\ominus} = \frac{Z_{N_s,1}}{Z_{N_s} V} \quad (23)$$

replaces the molecular configurational partition function z_i^0 for an ideal gas; see eqs 4 and 5. In eq 23, Z_{N_s} is the configurational partition function for pure solvent consisting of N_s molecules and $Z_{N_s,1}$ is the corresponding function in the presence of one solute molecule.

Furthermore, we take

$$\mu_i^{ex\ominus} = -k_B T \ln \frac{Z_{N_s,N_i+1}}{Z_{N_s,N_i} V z_i^{\ominus}} \quad (24)$$

By inspection, we see that eq 22 is equivalent to eq 1 and give the same μ_i in terms of the Z_{N_s,N_i} functions (both $z_i^{\ominus}$ and z_i^0 can be completely eliminated from these equations). The difference between eqs 1 and 22 is that $k_B T \ln(z_i^{\ominus}/z_i^0)$ has been subtracted from μ_i^0 to obtain $\mu_i^{\ominus}$ and added to μ_i^{ex} to obtain $\mu_i^{ex\ominus}$. Since the same quantity has been subtracted from μ_i^0 and added to μ_i^{ex}, their sum remains unchanged, so μ_i is also unchanged.

Note that $\mu_i^{ex\ominus} \to 0$ and hence $\gamma_i^{\ominus} \to 1$ when $c_i \to 0$ (i.e., $N_i \to 0$), which is the reason this choice of standard state is practical. As in the previous case, the concentration c_i^0 can assume any value. If the concentration c_i^0 is sufficiently low so that $\gamma_i^{\ominus} = 1$ to a very good approximation, $\mu_i^{\ominus}$ is the chemical potential of the actual solution with this concentration (this is exact in the limit $c_i^0 \to 0$). Otherwise, $\mu_i^{\ominus}$ is the chemical potential of a so-called hypothetical standard state that does not occur in reality (an "ideal dilute solution"). It is common to use the convention $c_i^0 = 1$ M, a truly hypothetical ideal dilute solution.

Equation 2 and the definitions of $\mu_i^{\ominus}$ and μ_i^0 imply

$$\mu_i^{\ominus} = \mu_i^0 + \mu_i^{ex}(N_i:\ 0 \to 1)$$

where the last term is the excess chemical potential calculated by adding one solute molecule to pure solvent. Thus, the standard chemical potential $\mu_i^{\ominus}$ for infinitely dilute solution can be obtained for any c_i^0 by calculating μ_i^0 for an ideal gas and by applying eq 2 to obtain $\mu_i^{ex}(N_i: 0 \to 1)$.

References and Notes

(1) Lyubartsev, A. P.; Martsinovski, A. A.; Shevkunov, S. V.; Vorontsov-Velyaminov, P. N. *J. Chem. Phys.* **1992**, *96*, 1776.
(2) Khare, A. A.; Rutledge, G. C. *J. Chem. Phys.* **1999**, *110*, 3063.
(3) Åberg, K. M.; Lyubartsev, A. P.; Jacobsson, S. P.; Laaksonen, A. *J. Chem. Phys.* **2004**, *120*, 3370.

(4) Lyubartsev, A. P.; Laaksonen, A.; Vorontsov-Velyaminov, P. N. *Mol. Simul.* **1996**, *18*, 43.

(5) Lyubartsev, A. P.; Laaksonen, A. *Comput. Phys. Comm.* **2000**, *128*, 565.

(6) Lyubartsev, A. P.; Laaksonen, A. EE Software; Stockholm University, Stockholm, Sweden.

(7) Rizzo, R. C.; Jorgensen, W. L. *J. Am. Chem. Soc.* **1999**, *121*, 4827.

(8) Values taken from the force field parameter library included in the *BOSS* software.[9−11]

(9) Jorgensen, W. L. *BOSS Software*, version 4.6; Yale University: New Haven, CT.

(10) Jorgensen, W. L. In *The Encyclopedia of Computational Chemistry*; Schleyer, P. v. R., Ed.; Wiley: New York, 1998; Vol. 5, p 3281.

(11) Jorgensen, W. L.; Tirado-Rives, J. *J. Comput. Chem.* **2005**, *26*, 1689.

(12) Storer, J. W.; Giesen, D. J.; Cramer, C. J.; Truhlar, D. G. *J. Comput.-Aided Mol. Des.* **1995**, *9*, 87.

(13) Udier-Blagovic, M.; Morales de Tirado, P.; Perlman, S. A.; Jorgensen, W. L. *J. Comput. Chem.* **2004**, *25*, 1322.

(14) Values taken from the force field parameter library included in the EE software.[5,6]

(15) Toukan, K.; Rahman, A. *Phys. Rev. B* **1985**, *31*, 2643.

(16) Andersson, J.; Ullo, J. J.; Yip, S. J. *Chem. Phys.* **1987**, *87*, 1726.

(17) Zacharias, M.; Straatsma, T. P.; McCammon, J. A. *J. Chem. Phys.* **1994**, *100*, 9025.

(18) Beutler, T. C.; Mark, A. E.; van Schaik, R. C.; Gerber, P. R.; van Gunsteren, W. F. *Chem. Phys. Lett.* **1994**, *222*, 529.

(19) Nose, S. *Mol. Phys.* **1984**, *52*, 255.

(20) Hoover, W. G. *Phys. Rev. A* **1985**, *31*, 1695.

(21) Allen, M. P.; Tildesley, D. J. *Computer Simulations of Liquids*; Clarendon: Oxford, 1987.

(22) Tuckerman, M. E.; Berne, B. J.; Martyna, G. J. *J. Chem. Phys.* **1992**, *97*, 1990.

(23) Lyubartsev, A. P.; Jacobsson, S. P.; Sundholm, G.; Laaksonen, A. *J. Phys. Chem. B* **2001**, *105*, 7775.